

Synthesis, Crystal Structure, and Magnetic Property of Delithiated Li_xMnO_2 ($x < 0.1$) Single Crystals: A Novel Disordered Rocksalt-Type Manganese Dioxide

Junji Akimoto,* Yasuhiko Takahashi, Yoshito Gotoh, and Kenji Kawaguchi

National Institute of Advanced Industrial Science and Technology (AIST), 1-1-1 Higashi, Tsukuba 305-8565, Japan

Kaoru Dokko and Isamu Uchida

Department of Applied Chemistry, Graduate School of Engineering, Tohoku University, Aramaki-Aoba 07, Aoba-ku, Sendai 980-8579, Japan

Received March 12, 2003. Revised Manuscript Received May 13, 2003

Single crystals of the chemically and electrochemically delithiated Li_xMnO_2 ($x < 0.1$) have been successfully synthesized from the parent orthorhombic LiMnO_2 single crystals. A single-crystal X-ray diffraction study revealed that the average structure of Li_xMnO_2 was the disordered rocksalt-type with the space group $Fm\bar{3}m$, and the lattice parameter $a = 4.095(3)$ Å. Some additional spots indicating the superlattice structure and diffuse scattering could be observed in the X-ray precession photographs. The mechanism of the structural transformation from the parent orthorhombic LiMnO_2 to the delithiated cubic Li_xMnO_2 was well explained by the manganese ion migration accompanied with Li^+ extraction. The magnetic properties of the chemically delithiated Li_xMnO_2 are compared with those of the parent LiMnO_2 . The extracted Curie constant in Li_xMnO_2 is consistent with the residual lithium content found analytically, as in the case of λ - MnO_2 .

Introduction

Layered lithium manganese oxides have attracted intense research interest as prospective cathode materials in secondary lithium batteries not only because of the low cost and low toxicity of manganese, but also because of their high theoretical capacities.^{1–4} LiMnO_2 is known to exist in two ordered rocksalt-type structures with orthorhombic and monoclinic symmetry, respectively. Orthorhombic LiMnO_2 has a zigzag layered β - NaMnO_2 type structure with the space group of $Pmnm$, as shown in Figure 1. The detailed crystal structure of this compound was deduced first from powder, and later from single-crystal, X-ray diffraction data.^{5–7} It is experimentally well-known that the structure of orthorhombic LiMnO_2 cathode transforms gradually and irreversibly into a spinel-type structure during several discharge–charge cycles.^{2,3} For practical reasons, such a structural change of electrodes is generally unfavorable, but in this case, the electrochemically generated spinel electrodes show significantly better

and more stable characteristics of the charge–discharge cycles than the regular spinel-type LiMn_2O_4 electrodes.

Recently, Tang et al.⁸ reported a structural-transformation model of orthorhombic LiMnO_2 to spinel-type LiMn_2O_4 accompanied by the Li^+ extraction. In contrast, Chiang et al.⁹ reported the role of cation disorder and transformation microstructures on electrochemical performance examined theoretically and experimentally. They predicted an intermediate structure with $Fm\bar{3}m$ space group between the parent orthorhombic structure with $Pmnm$ space group and the spinel-type structure with $Fd\bar{3}m$ space group, from the viewpoint of crystallographic considerations. However, such an intermediate structure could not be obtained experimentally as an average structure. To clarify the true crystal symmetry, precise crystal structure, and mechanism of the structure change in this intercalation system, the single-crystal X-ray diffraction method has been highly desired, as in the recent studies of the spinel-type $\text{Li}_{1-x}\text{Mn}_2\text{O}_4$.^{10–15}

* Corresponding author. E-mail: j.akimoto@aist.go.jp. Fax: +81-29-861-4803.

- (1) Armstrong, A. R.; Bruce, P. G. *Nature* **1996**, *381*, 499.
- (2) Ohzuku, T.; Ueda, A.; Hirai, T. *Chem. Express* **1992**, *7*, 193.
- (3) Gummow, R. J.; Liles, D. C.; Thackeray, M. M. *Mater. Res. Bull.* **1993**, *28*, 1249.
- (4) Shao-Horn, Y.; Hackney, S. A.; Armstrong, A. R.; Bruce, P. G.; Gitzendanner, R.; Johnson, C. S.; Thackeray, M. M. *J. Electrochem. Soc.* **1999**, *146*, 2404.
- (5) Johnston, W. D.; Heikes, R. R. *J. Am. Chem. Soc.* **1956**, *78*, 3255.
- (6) Dittrich, G.; Hoppe, R. *Z. Anorg. Allg. Chem.* **1969**, *368*, 262.
- (7) Hoppe, R.; Brachtel, G.; Jansen, M. *Z. Anorg. Allg. Chem.* **1975**, *417*, 1.

- (8) Tang, W.; Kanoh, H.; Ooi, K. *J. Solid State Chem.* **1999**, *142*, 19.
- (9) Chiang, Y.-M.; Wang, H.; Jang, Y.-I. *Chem. Mater.* **2001**, *13*, 53.
- (10) Akimoto, J.; Takahashi, Y.; Gotoh, Y.; Mizuta, S. *Chem. Mater.* **2000**, *12*, 3246.
- (11) Björk, H.; Gustafsson, T.; Thomas, J. O. *Electrochem. Commun.* **2001**, *3*, 187.
- (12) Tang, W.; Yang, X.; Kanoh, H.; Ooi, K. *Chem. Lett.* **2001**, 524.
- (13) Akimoto, J.; Takahashi, Y.; Gotoh, Y.; Mizuta, S. *J. Cryst. Growth* **2001**, *229*, 405.
- (14) Monge, M. A.; Amarilla, J. M.; Gutiérrez-Puebla, E.; Campa, J. A.; Rasines, I. *ChemPhysChem* **2002**, *3*, 367.

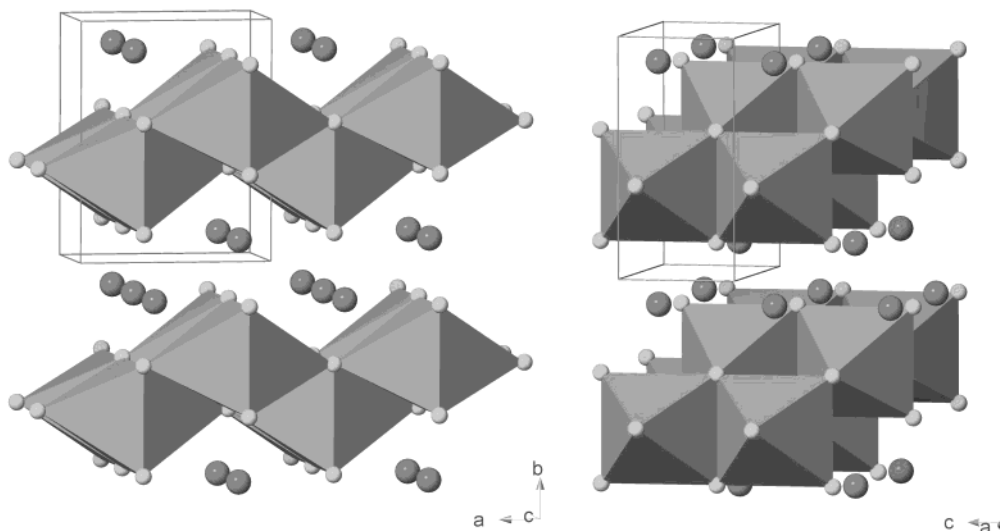


Figure 1. Crystal structure of orthorhombic LiMnO_2 .

The present paper has three main objectives. First, we prepare the electrochemically delithiated Li_xMnO_2 ($x < 0.1$) single crystals and determine the precise crystal structure by the single-crystal X-ray diffraction method. Second, we explain the mechanism of structural transformation by the manganese ion migration accompanied with Li^+ extraction. Finally, we demonstrate the magnetic property of the novel disordered rocksalt-type manganese dioxide compound obtained by the Li^+ extraction from the parent orthorhombic LiMnO_2 single crystals.

Experimental Section

Single-Crystal Synthesis. Single crystals of the orthorhombic LiMnO_2 were grown by a flux method, as mentioned previously.¹⁶ The as-prepared LiMnO_2 powder (Nippon Chemical Industrial Co., Ltd., Japan) was mixed with LiCl (99.9%) as a flux material in the nominal weight ratio of $\text{LiMnO}_2/\text{LiCl} = 1:10$. The flux growth was conducted in a vertical resistance furnace. The mixture was heated to 1273 K for 10 h in a sealed Pt tube, gradually cooled to 873 K, and then cooled naturally. The produced single crystals were easily separated from the frozen LiCl flux by rinsing the Pt tube in water for several hours.

Chemical Analysis. Chemical analyses of selected single-crystal specimens were carried out by SEM-EDX (JEOL JSM-5400). The chemical formulas of the samples were analyzed by inductively coupled plasma (ICP) spectroscopy using the pulverized single crystals (about 6 mg).

Electrochemical Delithiation. The controlled extraction of lithium from a piece of single crystal was achieved by electrochemical means using a microelectrode-based system.^{17–20} A selected LiMnO_2 crystal ($0.15 \times 0.03 \times 0.02 \text{ mm}^3$) was placed on a glass paper soaked in 1 M LiClO_4 /propylene carbonate (PC) + ethylene carbonate (EC) (1:1 vol) solution (Li-ion battery grade, Mitsubishi Kagaku Co.). A Pt–Rh fine filament (25 μm diam) was coated with a thin film of Teflon (Cytop, Asahi Glass), and was then cut to give a micro-disk electrode. The prepared microelectrode was held with x-y-z microposi-

tioner (Shimadzu MMS-77) and brought into contact with the LiMnO_2 crystal by handling the positioner under observation with a stereomicroscope (Nikon SMZ-U). The electrode potential was measured and controlled against a Li foil reference electrode with a potentiostat (Hokuto Denko HA-150). All the electrochemical experiments were conducted in a small drybox filled with air purified by a column (Balston 75-20, 203 K dew point).

The electrode potential was stepped from the open circuit potential (OCP, about 3.2 V) of LiMnO_2 to a desired value, such as 4.50 V vs Li. After the overnight electrolysis, the potentiostat was switched back to the OCP-measuring mode. We checked the completion of the extraction reaction with the stability of the regulated OCP, the value of which was 4.10 V vs Li. The obtained Li_xMnO_2 crystal was rinsed carefully with pure PC, and then supplied to the single-crystal X-ray diffraction analysis.

Chemical Delithiation. The Li_xMnO_2 single crystals were also prepared by a combined Li-ion extraction/chemical oxidation process. Selected LiMnO_2 single crystals were placed in 1 M HCl solution for several hours. No stirring or heating was performed. The obtained Li_xMnO_2 crystals were washed carefully with ethanol, and then supplied to chemical analysis, powder X-ray diffraction, and magnetic measurements.

Single-Crystal X-ray Diffraction. Crystals were examined with an X-ray precession camera (MoK α radiation filtered by Zr foil) to check on the crystal quality and to determine the lattice parameters, systematic extinctions, and possible superstructures. Integrated intensity data for the as-grown LiMnO_2 and the electrochemically delithiated Li_xMnO_2 single crystals were collected in the 2θ - ω scan mode at a scan rate of $1.0^\circ/\text{min}$ at 296 K on a Rigaku AFC-5S four-circle diffractometer (operating conditions 45 kV, 35 mA) using graphite-monochromatized MoK α radiation ($\lambda = 0.71073 \text{ \AA}$), and reduced to structure factors after due corrections for absorption and Lorentz and polarization effects. The lattice parameters of these compounds were determined by least-squares refinement using 2θ values of 25 strong reflections in the range 20 – 30° and MoK α ($\lambda = 0.71073 \text{ \AA}$) on the four-circle diffractometer.

Powder X-ray Diffraction. The X-ray powder diffraction profiles were measured using a Rigaku RINT2550 diffractometer (operating conditions 40 kV, 200 mA) with CuK α radiation equipped with a curved graphite monochromator. The d spacing measurements were performed at 2.0° (2θ) min^{-1} in the range of $10^\circ < 2\theta < 80^\circ$ using powdered single crystals. Lattice parameters were calculated by a least-squares method.

Magnetic Measurements. The temperature dependence of the magnetic susceptibility was measured with a SQUID magnetometer (Quantum Design, MPMS) in a temperature

(15) Takahashi, Y.; Akimoto, J.; Gotoh, Y.; Dokko, K.; Nishizawa, M.; Uchida, I. *J. Phys. Soc. Jpn.* **2003**, *72*, 1483.

(16) Strobel, P.; Levy, J.-P.; Joubert, J.-C. *J. Cryst. Growth* **1984**, *66*, 257.

(17) Uchida, I.; Fujiyoshi, H.; Waki, S. *J. Power Sources* **1997**, *68*, 139.

(18) Nishizawa, M.; Uchida, I. *Electrochim. Acta* **1999**, *44*, 3629.

(19) Nishizawa, M.; Koshika, H.; Hashitani, R.; Itoh, T.; Abe, T.; Uchida, I. *J. Phys. Chem. B*, **1999**, *103*, 4933.

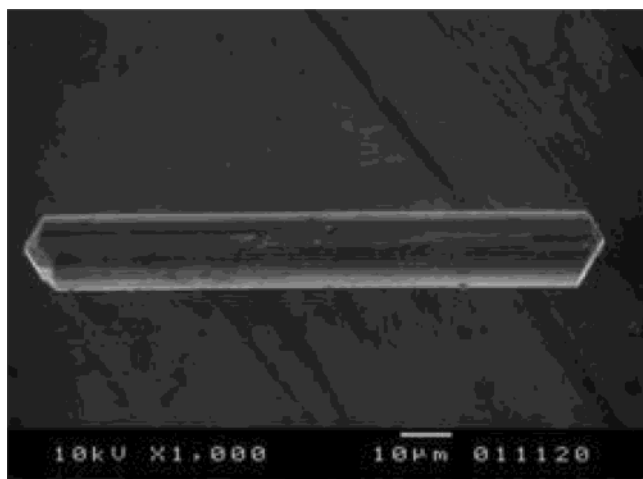


Figure 2. SEM photograph of as-grown LiMnO_2 single crystal.

range from 4.5 to 300 K at applied fields of 10, 20, and 100 Oe. Diamagnetic corrections for magnetic susceptibilities were taken into account.

Results and Discussion

LiMnO_2 . Black, needlelike LiMnO_2 single crystals of about $0.15 \times 0.03 \times 0.02 \text{ mm}^3$ in average were obtained, as shown in Figure 2. EDX analysis showed that the crystals were free from platinum contamination from the vessel. The chemical formula, analyzed by ICP, was $\text{Li}_{1.0}\text{Mn}_{1.0}\text{O}_2$, which is consistent with the result of the present structure refinement.

Precession photographs indicate the as-grown LiMnO_2 belongs to the orthorhombic system with the space group $Pnmm$, as in the previous work.⁷ Figure 3 shows the $\{h0l\}^*$ and $\{0kl\}^*$ precession photographs of the LiMnO_2 single crystal, taken at room temperature. No additional spots indicating the ordered structure and diffuse scattering could be observed in these photographs. The lattice parameters for the as-grown LiMnO_2 were identical with those in the previous report.^{7,16}

The structure refinement for orthorhombic LiMnO_2 was carried out with the atomic coordinates reported in the literature.⁷ The converged final R and wR values and other experimental and crystallographic data are summarized in Table 1. Difference Fourier syntheses using the final atomic parameters showed no significant residual peaks. The final atomic coordinates and displacement parameters are given in Table 2. All calculations were carried out using the Xtal3.4 package program.²¹ The refined structural parameters are in excellent agreement with those in the previous reports for LiMnO_2 .⁷

Magnetic susceptibility was measured as a function of temperature at fixed fields using the present LiMnO_2 single-crystal samples. Figure 4 shows a typical temperature dependence from 5 to 300 K at 100 Oe. The open and filled marks correspond to measurements on field cooling and on heating after zero-field cooling, respectively. The history dependence of temperature

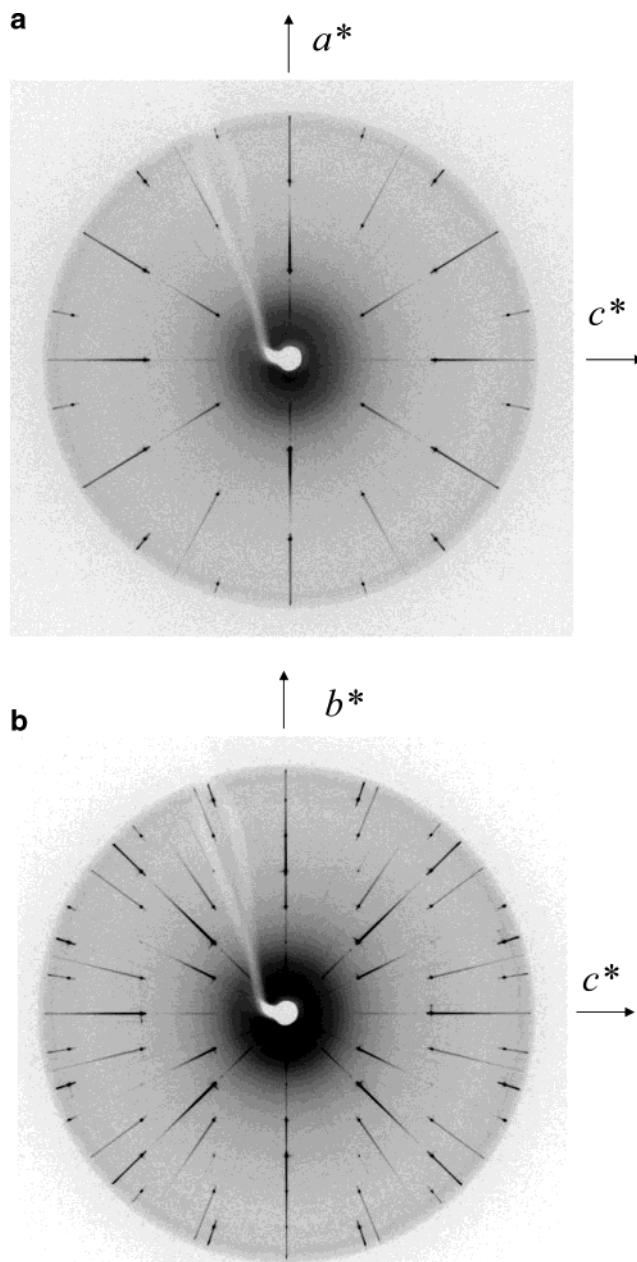


Figure 3. (a) $\{h0l\}^*$ and (b) $\{0kl\}^*$ precession photographs of as-grown orthorhombic LiMnO_2 single crystal. $\text{MoK}\alpha$ radiation filtered by Zr foil was used.

versus M/H maximum below 50 K was clearly observed. Similar features were observed previously in the LiMnO_2 polycrystalline sample.²²

From the results of the present structural and magnetic characterization, we confirmed that the present single-crystal sample had a stoichiometric LiMnO_2 chemical composition.

Li_xMnO_2 ($x < 0.1$). Figure 5 shows a SEM photograph of the electrochemically delithiated Li_xMnO_2 single crystal. Compared with that of the parent LiMnO_2 , the crystal becomes fragile, and there are many surface grooves parallel to the needle direction. The color of the crystals changed from black to brown by Li^+ extraction.

(20) Dokko, K.; Nishizawa, M.; Mohamedi, M.; Umeda, M.; Uchida, I.; Akimoto, J.; Takahashi, Y.; Gotoh, Y.; Mizuta, S. *Electrochem. Solid State Lett.* **2001**, *4*, A151.

(21) Hall, S. R.; King, G. S. D.; Stewart, J. M., Eds. *Xtal3.4 User's Manual*. University of Western Australia: Lamb, Perth, 1995.

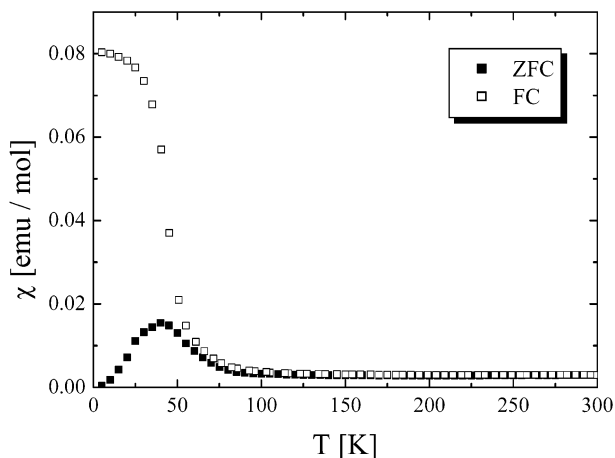
(22) Greedan, J. E.; Raju, N. P.; Davidson, I. J. *J. Solid State Chem.* **1997**, *128*, 209.

Table 1. Experimental and Crystallographic Data for Orthorhombic LiMnO_2

formula	LiMnO_2
crystal system	orthorhombic
space group	$Pnmm$ (no. 59)
lattice parameters	
a (Å)	4.574(1)
b (Å)	5.752(1)
c (Å)	2.808(1)
V (Å ³)	73.86(3)
crystal size (mm)	$0.13 \times 0.03 \times 0.03$
temperature (K)	296
scan type	$2\theta - \omega$
scan speed (°/min)	1.0
maximum 2θ (°)	70
absorption correction	Gaussian integration
transmission factors	
min.	0.760
max.	0.795
measured reflections	978
R_{int} (%)	1.06
independent observed reflections	207
number of variables	18
R (%)	1.30
wR [$w = 1/\sigma^2 F$] (%)	1.57

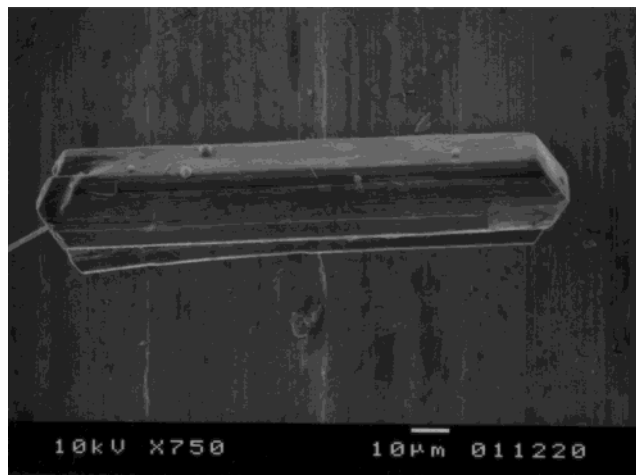
Table 2. Structural Parameters for Orthorhombic LiMnO_2

atom	x	y	z	U_{eq} (Å ²)
Li	1/4	0.1161(7)	1/4	0.010(2)
Mn	1/4	0.63477(6)	1/4	0.0043(2)
O1	3/4	0.1423(3)	1/4	0.0068(7)
O2	3/4	0.5993(3)	1/4	0.0058(7)

**Figure 4.** Temperature dependence of the magnetic susceptibility for as-grown LiMnO_2 single crystals measured at $H = 100$ Oe after zero-field cooling (filled symbols) and on-field cooling (open symbols).

The chemical formula of the electrochemically delithiated single crystal was roughly estimated (from the OCP value) to be $\text{Li}_{0.1}\text{MnO}_2$. The chemical composition of the chemically delithiated crystals, analyzed by ICP, was $\text{Li}_{0.06}\text{Mn}_{1.0}\text{O}_2$. The value is well consistent with that obtained by the electrochemical delithiation. The chemical formula of both the electrochemically and chemically delithiated compounds is hereafter denoted as Li_xMnO_2 , where the lithium content, x , is less than 0.1.

Precession photographs indicate the average structure of the electrochemically delithiated Li_xMnO_2 belongs to the cubic system with the space group $Fm\bar{3}m$. Figure 6 shows the $\{hko\}^*$ and $\{hhl\}^*$ precession photographs of the electrochemically delithiated Li_xMnO_2 single crystal, taken at room temperature. Some additional

**Figure 5.** SEM photograph of electrochemically delithiated Li_xMnO_2 single crystal.**Table 3. Experimental and Crystallographic Data for Cubic Li_xMnO_2**

structural formula	MnO_2
crystal system	cubic
space group	$Fm\bar{3}m$ (no. 225)
lattice parameters	
a (Å)	4.095(3)
V (Å ³)	68.67(15)
crystal size (mm)	$0.18 \times 0.02 \times 0.02$
temperature (K)	296
scan type	$2\theta - \omega$
scan speed (°/min)	1.0
maximum 2θ (°)	70
absorption correction	Gaussian integration
transmission factors	
min.	0.532
max.	0.845
measured reflections	55
R_{int} (%)	6.2
independent observed reflections	18
number of variables	4
R (%)	6.4
wR [$w = 1/\sigma^2 F$] (%)	6.7

spots indicating the superlattice structure and diffuse scattering could be observed in these photographs (Figure 7). This fact suggests the ordered local structure or short-range ordering in the single crystal specimen, as previously observed by electron diffraction study.⁹ However, these reflections were very weak in intensity compared with the main Bragg reflections. Therefore, we can describe the average structure as disordered rocksalt-type. The lattice parameter for the cubic rocksalt-type structure model was determined to be $a = 4.095(3)$ Å using a four-circle diffractometer. The value is considerably different from those in the disordered rocksalt-type MnO ($a = 4.446(1)$ Å) and the spinel-type $\lambda\text{-MnO}_2$ ($a = 4.02 \times 2$ Å).^{23,24}

The structure refinement for the electrochemically delithiated Li_xMnO_2 was carried out with the disordered rocksalt-type atomic coordinates and the space group $Fm\bar{3}m$. The converged final R and wR values and other experimental and crystallographic data are summarized in Table 3. Difference Fourier syntheses using the final atomic parameters showed no significant residual peaks,

(23) Sasaki, S.; Fujino, K.; Takéuchi, Y.; Sadanaga, R. *Acta Crystallogr., Sect. A* **1980**, *36*, 904.

(24) Greedan, J. E.; Raju, N. P.; Wills, A. S.; Morin, C.; Shaw, S. M. *Chem. Mater.* **1998**, *10*, 3058.

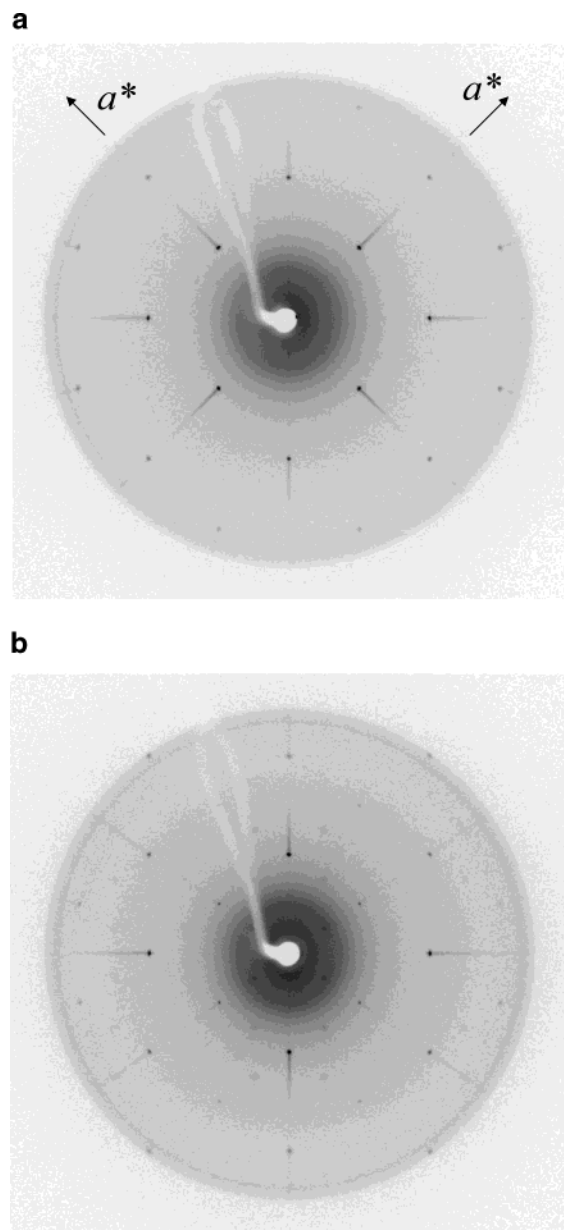


Figure 6. (a) $\{hk0\}^*$ and (b) $\{hhl\}^*$ precession photographs of electrochemically delithiated cubic Li_xMnO_2 single crystal. $\text{MoK}\alpha$ radiation filtered by Zr foil was used.

Table 4. Structural Parameters for Cubic Li_xMnO_2

atom	x	y	z	$U_{\text{eq.}} (\text{\AA}^2)$	sof
Mn	0	0	0	0.014(2)	0.48(3)
O	1/2	1/2	1/2	0.033(5)	1

suggesting Li atoms. The final atomic coordinates and displacement parameters are given in Table 4. The refined occupancy parameter for Mn, the value of which is 48%, is well consistent with the chemical analysis. The derived Mn–O distance of 2.048(2) Å is longer than that expected for Mn^{4+} . However this can be explained by about 50% vacancy of the Mn site.

Figure 8 compares the X-ray powder diffraction patterns of as-grown orthorhombic LiMnO_2 crystals and the chemically delithiated Li_xMnO_2 crystals. The cubic lattice parameter of Li_xMnO_2 , determined by a least-squares refinement using the powder data, was $a = 4.088(6)$ Å. As in the present single-crystal X-ray study, the (111) peak of the cubic spinel structure at around

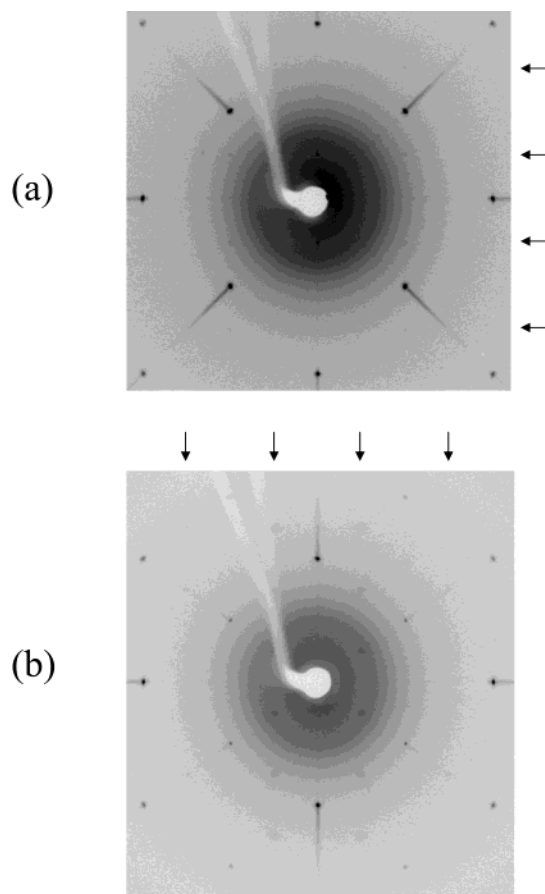


Figure 7. Magnified photographs of the center regions of (a) $\{hk0\}^*$ and (b) $\{hhl\}^*$ precession photographs shown in Figure 6. Some additional spots indicating the superlattice structure and diffuse scattering are indicated by arrows.

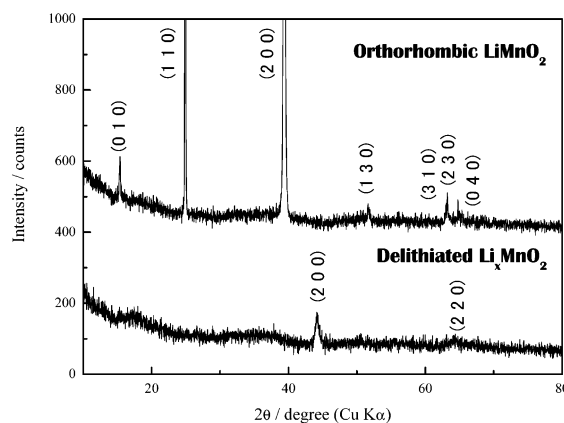


Figure 8. X-ray powder diffraction patterns of as-grown LiMnO_2 single crystals and the chemically delithiated Li_xMnO_2 single crystals. The correction for preferred orientation caused by their needlelike crystal shapes was not performed.

19° in 2θ could not be observed in this pattern. Therefore, the average structure of the chemically delithiated sample also can be described as the disordered rocksalt-type structure.

Magnetic susceptibility was measured as a function of temperature at fixed fields using the chemically delithiated Li_xMnO_2 single-crystal samples. Figure 9 shows a typical temperature dependence from 5 to 300 K at 100 Oe. The open and filled marks correspond to measurements on field cooling and on heating after zero-field cooling, respectively. A sharp maximum appears

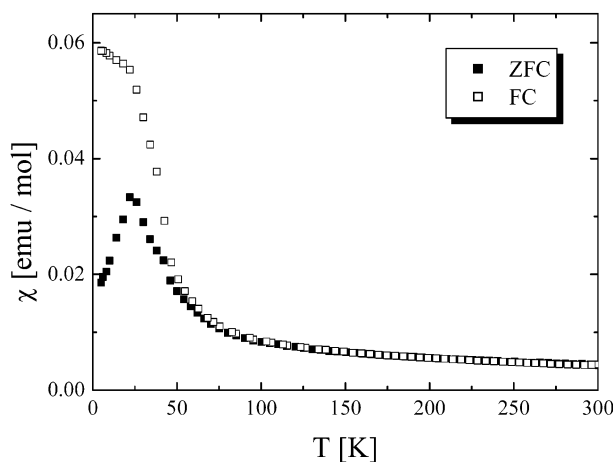


Figure 9. Temperature dependence of the magnetic susceptibility for the chemically delithiated Li_xMnO_2 single crystals measured at $H = 100$ Oe after zero-field cooling (filled symbols) and on-field cooling (open symbols).

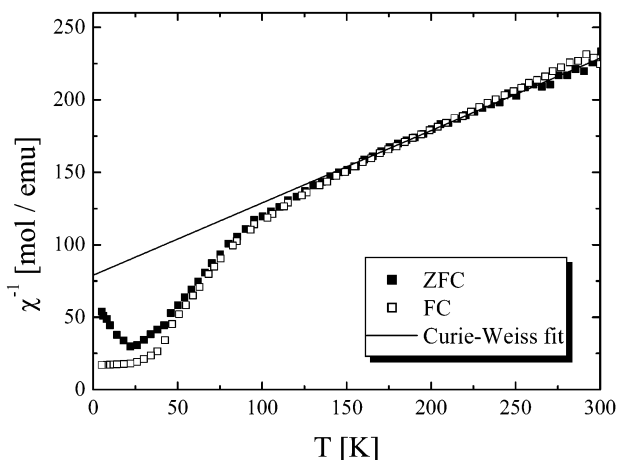


Figure 10. Inverse magnetic susceptibility for the chemically delithiated Li_xMnO_2 single crystals. The Curie-Weiss fit is indicated.

at 24 K in the ZFC magnetization, and an abrupt increase of the FC magnetization is noticeable with decreasing temperature below 50 K, indicating the presence of a ferromagnetic component. The origin of the ferromagnetic component in Li_xMnO_2 is not clear. The complex magnetic behavior may come from the contribution of $90^\circ \text{Mn}^{4+}-\text{O}^{2-}-\text{Mn}^{4+}$ ferromagnetic interaction reported by Blasse.²⁵ However, as ferromagnetism is also observed in the parent LiMnO_2 (Figure 4),²² it may be caused by a small amount of magnetic impurity. To confirm this phenomenon, further magnetic properties below 24 K should be measured using higher quality samples.

The inverse susceptibility is plotted in Figure 10, including a Curie-Weiss law fit to the data above 150 K. The extracted Weiss temperature and Curie constant are $\theta = -158$ K and $C = 2.00$ emu K/mol, respectively. A negative Weiss temperature indicates antiferromagnetic interaction between Mn^{4+} spins. From the Curie constant, the effective moment is determined to be $\mu_{\text{eff}} = 4.00 \mu_B$, which is slightly larger than the theoretical spin only value of $3.87 \mu_B$ for Mn^{4+} ($S = 3/2$). This

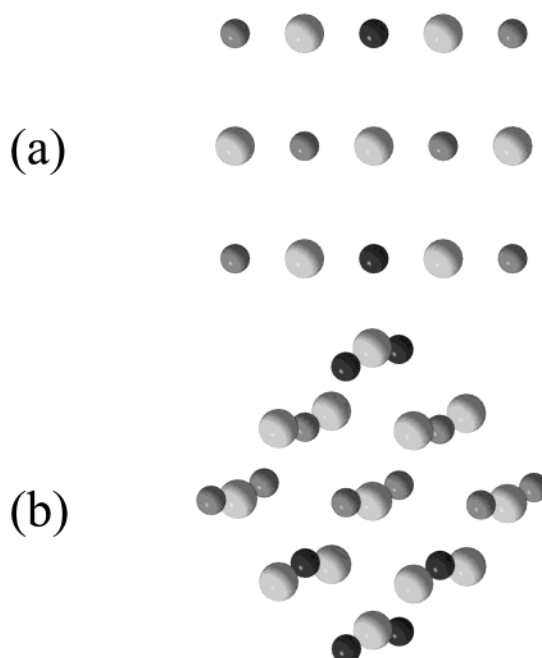


Figure 11. Rocksalt-type atomic arrangements in the parent orthorhombic LiMnO_2 structure, viewed along (a) [010] and (b) [100] directions. The gray, black, and white balls correspond to the Li, Mn, and O atoms, respectively.

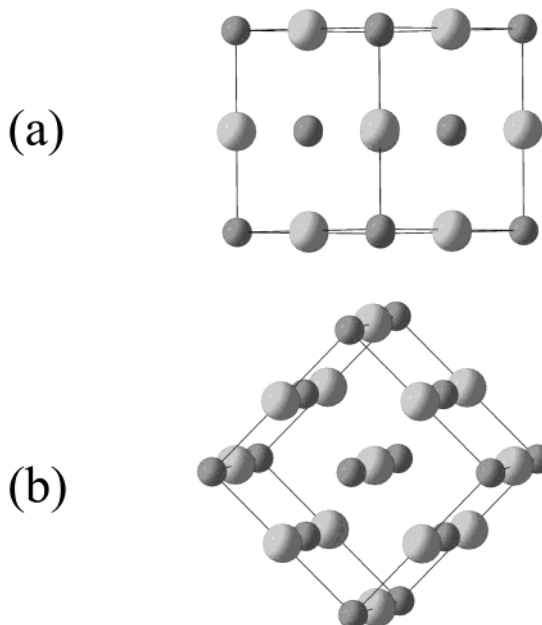


Figure 12. Rocksalt-type atomic arrangements in the delithiated cubic MnO_2 structure, viewed along (a) [110] and (b) [100] directions. The gray and white balls correspond to the Mn and O atoms, respectively.

fact is consistent with the chemical analysis results that show a lithium content of 6%, which implies an equivalent concentration of Mn^{3+} ($S = 2$). Previously, Greedan et al. reported $\mu_{\text{eff}} = 3.97 \mu_B$ for the spinel-type $\lambda\text{-MnO}_2$ samples prepared by a similar chemical delithiation technique.²⁴ From these facts, we can be fairly certain that a novel disordered rocksalt-type MnO_2 can be prepared by delithiation from the orthorhombic LiMnO_2 .

Structural Transformation Mechanism. The present single-crystal X-ray diffraction study revealed the structure change together with lithium extraction reaction from the parent orthorhombic zigzag-layered struc-

(25) Blasse, G. *J. Phys. Chem. Solids* **1966**, 27, 383.

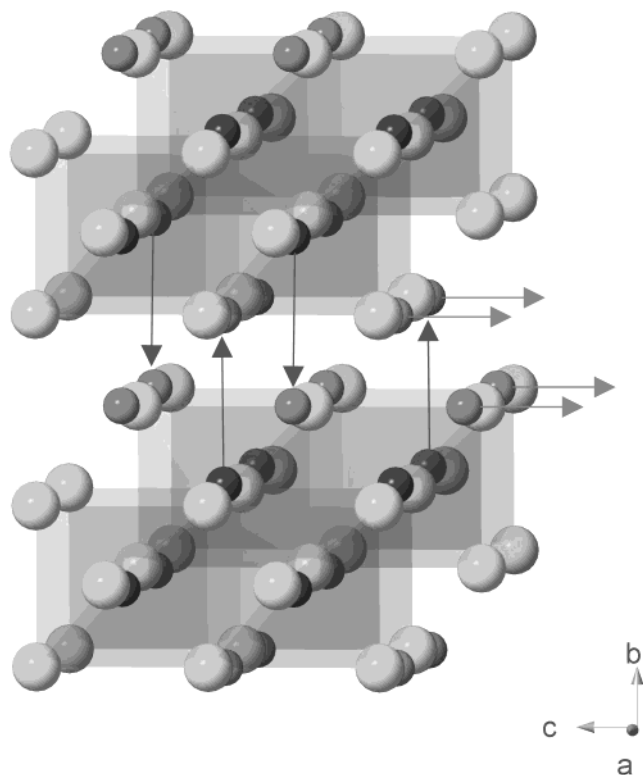


Figure 13. Atomic migration model for Li (arrows) and Mn (arrows) atoms from the orthorhombic LiMnO_2 structure to the cubic rocksalt-type MnO_2 structure. The balls correspond to the Li, Mn, and O atoms, respectively. The MnO_6 are drawn with the octahedra. Atomic migration model for Li (gray arrows) and Mn (black arrows) atoms from the orthorhombic LiMnO_2 structure to the cubic rocksalt-type MnO_2 structure. The gray, black, and white balls correspond to the Li, Mn, and O atoms, respectively. The MnO_6 are drawn with the transparent octahedra.

ture to the cubic disordered rocksalt-type one. Because of the characteristic and anisotropic morphology of the starting single-crystal specimen, we have successfully pursued the mechanism of structural transformation by using single-crystal X-ray diffraction photographs.

The parent orthorhombic LiMnO_2 has a zigzag layered structure, as mentioned above (Figure 1). On the other hand, this structure can be also described as a cubic closest packing for oxygen atoms, in which both of the Li and Mn atoms occupy the octahedral O_6 interstices. Figure 11 shows the rocksalt-type atomic arrangement in the parent LiMnO_2 structure. Each view direction in Figure 11(a) and (b) corresponds to the X-ray photographs shown in Figure 3(a) and (b), respectively. Similarly, the ideal rocksalt-type atomic arrays (Figure 12(a) and (b)) correspond to the directions of the X-ray photographs of the electrochemically delithiated single crystal shown in Figure 6(a) and (b), respectively. It should be emphasized that we have taken the X-ray photographs (Figures 3 and 4) from the same direction to the crystal shape (Figures 2 and 5). Namely, the incident directions of X-ray to the characteristic crystal faces in Figure 11(a) and (b) are the same as those in Figure 12(a) and (b), respectively. From these facts, we can easily understand that this structure change is not caused by oxygen rearrangement and has been achieved

by the migration of not only all of the lithium ions but also half of the manganese ions, as summarized in Figure 13. First, all of the Li^+ migrates out of the lattice by the electrochemical potential, resulting in the formation of vacant octahedral sites (gray arrows in Figure 13). Then, half of the manganese ions migrate statistically into the vacant octahedral sites (black arrows in Figure 13). Accordingly, the migration of metal ions has accompanied a slight shift for oxygen atoms to the ideal CCP positions, resulting in the cubic symmetry. We think that the manganese ion migration could be caused by the structural instability of the "zigzag layered MnO_2 ".

Conclusion

The present single-crystal X-ray diffraction study revealed the structure change together with lithium extraction reaction from the parent orthorhombic zigzag-layered LiMnO_2 structure to the cubic disordered rocksalt-type Li_xMnO_2 with $x < 0.1$. The single-crystal to single-crystal transformation has been confirmed by the single-crystal X-ray precession method. The disordered rocksalt-type structure was previously predicted from a viewpoint of crystallographic phase transformation. In the present study, the metastable phase has been obtained as a single-crystal form for the first time.

On the other hand, low-temperature synthetic techniques called "chimie douce" have resulted in major developments in the solid state chemistry of transition metal oxides. The systematic study of oxide bronzes in the period 1950–1980 paved the way to further advances in the solid state chemistry of oxides, including the alkali metal intercalation–deintercalation chemistry by soft chemistry or electrochemical methods. These techniques also gave access to new metastable compounds such as $\lambda\text{-MnO}_2$ ²⁶ and several new forms of TiO_2 .^{27–29} In the present study, we report a novel disordered rocksalt-type manganese dioxide, prepared by the electrochemical and chemical delithiation from the parent orthorhombic LiMnO_2 .

It should be noted that it is not clear from the present work whether the rocksalt-type form of MnO_2 can be stabilized without finite amounts of Li^+ , as in the case of $\lambda\text{-MnO}_2$. The superlattice spots and diffuse scattering observed in the present single-crystal X-ray study may be caused by the remaining lithium ions. Further soft chemical studies for the LiMnO_2 crystals and polycrystalline samples should be carried out. We believe that the disordered rocksalt-type structure is a key to understanding the good and stable characteristics of the charge–discharge cycles in the LiMnO_2 electrodes for the battery use.

CM034147B

(26) Hunter, J. C. *J. Solid State Chem.* **1981**, 39, 142.

(27) Marchand, R.; Brohan, L.; Tournoux, M. *Mater. Res. Bull.* **1980**, 15, 1129.

(28) Latroche, M.; Brohan, L.; Marchand, R.; Tournoux, M. *J. Solid State Chem.* **1989**, 81, 78.

(29) Akimoto, J.; Gotoh, Y.; Oosawa, Y.; Nonose, N.; Kumagai, T.; Aoki, K.; Takei, H. *J. Solid State Chem.* **1994**, 113, 27.